Physicochemical, pharmacokinetic and pharmacodynamic analyses of amphiphilic cyclodextrin-based nanoparticles designed to enhance intestinal delivery of insulin

Elena Presas, Fiona McCartney, Eric Sultan, Corina Hunger, Sabine Nellen, Clara V. Alvarez, Ulrich Werner, Didier Bazile, David J. Brayden, Caitriona M. O'Driscoll

PII: S0168-3659(18)30448-6
DOI: doi:10.1016/j.jconrel.2018.07.045
Reference: COREL 9405

To appear in: *Journal of Controlled Release*

Received date: 23 March 2018
Revised date: 11 July 2018
Accepted date: 29 July 2018

Please cite this article as: Elena Presas, Fiona McCartney, Eric Sultan, Corina Hunger, Sabine Nellen, Clara V. Alvarez, Ulrich Werner, Didier Bazile, David J. Brayden, Caitriona M. O'Driscoll , Physicochemical, pharmacokinetic and pharmacodynamic analyses of amphiphilic cyclodextrin-based nanoparticles designed to enhance intestinal delivery of insulin. Corel (2018), doi:10.1016/j.jconrel.2018.07.045

Physicochemical, pharmacokinetic and pharmacodynamic analyses of amphiphilic cyclodextrin-based nanoparticles designed to enhance intestinal delivery of insulin

*Elena Presas[1], Fiona McCartney[2], Eric Sultan[3], Corina Hunger[3], Sabine Nellen[3], Clara V. Alvarez[4], Ulrich Werner[2], Didier Bazile[3], David J. Brayden[2], Caitriona M. O'Driscoll[1]**

[4]Centre for Investigations in Molecular Medicine and Chronic Disease (CIMUS) and Institute of Investigaciones Sanitarias (IDIS), Group of Endocrine Neoplasia and Differentiation, University of Santiago de Compostela (USC), Santiago de Compostela, Spain.
[3]Sanofi Research and Development
[2]Veterinary Sciences Centre and Conway Institute, University College Dublin, Ireland
[1] Pharmacodelivery Group, School of Pharmacy, University College Cork, Cork, Ireland
**corresponding author: caitriona.odriscoll@ucc.ie*

ABSTRACT

Due to excellent efficacy, low toxicity, and well-defined selectivity, development of new injectable peptides is increasing. However, the translation of these drugs into products for effective oral delivery has been restricted due to poor oral bioavailability. Nanoparticle (NP) formulations have potential to overcome the barriers to oral peptide delivery through protecting the payload and increasing bioavailability. This study describes the rational design, optimization and evaluation of a cyclodextrin-based NP entrapping insulin glulisine for intestinal administration. A cationic amphiphilic cyclodextrin (click propyl-amine cyclodextrin (CD)) was selected as the primary complexing agent for NP development. Following NP synthesis, *in vitro* characterization was performed. The insulin glulisine NPs exhibited an average size of 109 ± 9 nm, low polydispersity index (0.272) negative zeta potential (-25 ± 3 mV), high association efficiency (71.4 ± 3.37 %) and an insulin loading of 10.2 %. In addition, the NPs exhibited colloidal stability in intestinal-biorelevant media (SIF, supplemented-SIF 1 % (w/v) and FaSSIF-V2) for up to 4 hours. Proteolysis studies indicated that the NPs conferred protection to the entrapped insulin relative to free insulin. *In vivo* rat jejunal instillation studies demonstrated that the NPs mediated systemic insulin absorption, accompanied by a decrease in blood glucose levels. The relative bioavailability of the instilled insulin (50 I.U./kg) from the NP was 5.5 % compared to subcutaneous administration of insulin solution (1 I.U. /kg). The pharmacodynamic and pharmacokinetic data indicate that this cyclodextrin-based formulation may have potential for further research as an oral insulin dosage form.

Keywords: nanoparticles, cyclodextrin, insulin, oral protein delivery

INTRODUCTION

The number of proteins and peptide-like drugs in the pharmaceutical industry's pipeline has been increasing in recent years due to significant therapeutic efficacy and exceptional selectivity (1). The capacity to administer these drugs via a non-invasive route remains a key challenge for formulation scientists. While oral administration remains the preferred option, low oral bioavailability due to poor intestinal permeability and pre-systemic degradation by proteolytic enzymes hampers administration via this route (2). In addition, poor patient compliance often results from complications associated with injectable chronic treatments including pain and side effects at the injection site (3). Another potential advantage of orally-administered insulin for *diabetes mellitus* is that insulin absorbed from the intestine would travel directly to the liver via the hepatic portal vein before reaching the peripheral tissues, thus simulating the physiological secretion pattern of the pancreas and potentially decreasing side effects associated with subcutaneous administration (4).

Different approaches have been explored to enhance oral bioavailability of insulin, including the chemical modification of insulin, co-administration with absorption enhancers and/or enzyme inhibitors and the formulation of insulin into particulates (reviewed in (5)). However, to date, an effective insulin oral delivery system has yet to be achieved. Recently, interest in the development of oral nanocarriers based on the use of biodegradable and biocompatible polymers has grown due to the advantages associated with these systems. Nanoparticle formulations can protect the peptide and can potentially carry pay-load across small intestinal mucus to the epithelium thereby improving bioavailability (6, 7).

The current work aims to design and optimise a nanoparticle formulation based on chemically-modified cyclodextrins (CDs) in combination with insulin glulisine (a rapidly acting insulin analogue developed by Sanofi-Aventis (Paris))(8). CDs can rearrange into supramolecular assemblies, which stabilize the drug and increases the interaction with biological membranes resulting in enhanced membrane permeability. Such properties make CDs an interesting formulation approach for oral peptide delivery (9). An amphiphilic cationic CD ("click propyl-amine CD") was selected as a primary complexing agent. This CD was previously synthesised using 'click' chemistry to selectively modify the primary side with lipid chains (SC_{12}) and the secondary side with cationic propyl-amine groups (10).

In order to improve the stability and the muco-penetration properties of the nanoparticle formulation, two additional excipients were included: a PEGylated phospholipid [1,2-distearoyl-sn-glycero-3-phosphoethanolamine–N-[methoxy(polyethylene glycerol)-2000] or mDSPE PEG 2000 and a negatively-charged polymer (dextran sulphate). In parallel with the selection of the nanoparticle composition, the method of preparation was optimized to achieve: i) reproducibility of the nanoparticle physico-chemical properties with maximal insulin loading efficiency; ii) stability of the nanostructure and insulin upon contact with bio-relevant intestinal media; and iii) enhanced permeability of insulin through the intestinal epithelium. Finally, the pharmacokinetic and pharmacodynamic profiles of the optimised prototype were evaluated *in vivo* in rats following intestinal instillation.

MATERIALS AND METHODS

2.1. Materials

Insulin glulisine was kindly provided by Sanofi (Paris) (11). Click propyl-amine CD was synthetized as previously described (12, 13). mPEG-DSPE MW 2000 was acquired from Nano CS (NY, USA). Dextan sulphate sodium salt from *Leuconostoc spp*. (Mol.Wt. ~ 5000 g/mol), aprotinin from bovine lung (lyophilized powder, 3-8 TIU/mg solid), N,N,N',N-Tetramethylethylenediamine (TEMED, bioreagent, suitable for electrophoresis, ~99 %), monobasic potassium phosphate (KH_2PO_4), pancreatin from porcine pancreas (4 x United States Pharmacopeia (USP) specifications) and Coomassie brilliant blue R were adquired from Sigma-Aldrich (Wicklow, Ireland). In addition, acrylamide/bis Acrylamide (bioReagent, suitable for electrophoresis, 30 % solution), sodium hydroxide (NaOH 1M) and hydrogen chloride (HCL, bioReagement, for molecular biology, 36.5-38 %) Trizma® base (BioUltra, for molecular biology, ≥99.8%), glycine (for electrophoresis, ≥99%) and ammonium persulfate ($(NH_4)2S_2O_8$, ≥98%) were purchased from Sigma-Aldrich (Wicklow, Ireland).

2.2. Circular dichroism measurements

Circular dichroism spectras were recorded in triplicate using a Chirascan™ spectrophotometer (Applied Photophysics, Surrey, UK), using 40 µL of sample (insulin glulisine solution or insulin glulisine NPs solution at different concentrations depending on the assay) in a 0.01 mm quartz cell, at a scanning speed of 1 nm/s (180 to 260 nm). Sample temperature was set at 20°C using a Quantum temperature control device (Quantum Northwest TC 125™ Temperature Controller WA, USA). Sample backgrounds were recorded and subtracted from the different samples. A 5-pt curve smoothing was applied to the averaged spectra after baseline subtraction. In addition, the CDNN analysis was performed in order to deconvolute the CD spectra and evaluate the contribution of the different protein segments (14).

2.3. Preparation of the click propyl-amine cyclodextrin: insulin glulisine nanocomplexes

Click propyl-amine CD was weighed and dissolved in chloroform at a concentration of 1 µg/µL. The solvent was evaporated under a continuous stream of nitrogen. The CD film was reconstituted in deionised water and the solution was sonicated for 60 min. Insulin glulisine was dissolved in HCL 0.01 M (1 µg/µL). A range of nanocomplexes with different molar ratios between the insulin glulisine: click propyl-amine CD (1:3; 1:7 and 1:14) were prepared as follows: the protein solution was added to different volumes of click propyl-amine CD to obtain the different molar ratios for the drug cargo: cyclodextrin. The pH values of the different formulations were adjusted to 6.5.

2.4. *Evaluation of the binding efficiency of the click propyl-amine cyclodextrin*

The binding efficiency of the click propyl-amine CD was analysed by native-polyacrylamide gel electrophoresis (PAGE electrophoresis) (15). Briefly, the nanocomplexes were prepared as detailed in *Section 2.3*. Different nanocomplexes at various molar ratios (cyclodextrin: insulin glulisine) and the corresponding controls were loaded at the same concentration onto a Trys-glicine gel with the separating gel of 10 % acrylamide and the staking gel of 5% of acrylamide. The loading buffer (1x) was added to the samples in a volume ratio of 4:1 (samples: loading buffer). Electrophoresis was performed at 90 V for 1 h. After the process, gels were stained with 0.1 % Coomassie brilliant blue for 30 min and detained overnight

with a solution of 20 % of methanol and 10 % of acetic acid. Images were examined using *ImageJ®* software (NIH; USA).

2.5. Preparation of insulin glulisine following the layer-by-layer technique

Click propyl-amine CD was dissolved acording to *Section 2.3* at a concentration of 5 µg/µL. Insulin glulisine was dissolved in HCL 0.01 M (5 µg/µL) and added to a solution of click propyl-amine CD at pH 6.5, vortexed for 30 seconds followed by horizontal stirring for 10 min (300 rpm, RT Thermomixer confort, thermomixer R. Eppendorf. Sigma-Aldrich). This process was followed by the post-insertion of mPEG-DSPE 2000. The phospholipid was weighed and dissolved in chloroform and the organic solvent was evaporated under a continuous stream of nitrogen. The resulting phospholipid film was reconstituted in HEPES buffer at pH 7.4 to achieve a final concentration of mPEG-DSPE 2000 of 10 µg/µL (65 °C, 20 min). The incubation procedure was repeated with the PEGylated phospholipid (37 ° C, 20 min). Finally, a coating of dextran sulphate was added to the nanocomplex by incubating the NPs with a solution of the polymer (7.5 µg/µL) for 10 min.

2.6. Physicochemical characterization of the nanostructures

The hydrodynamic diameter and polydispersity index (PdI) were measured by photon correlation spectroscopy (PCS). Zeta potential was determined by laser-Doppler anemometry (Zetasizer®, NanoZS, Malvern Instruments, Malvern, UK). Samples were measured following dilution in distilled water (1:10).

2.7. Morphological evaluation

2.7.1. Transmission electron microscopy (TEM)

Formulations were added to a 400-mesh carbon-film copper grid for three minutes, and the excess formulation was blotted using filter paper. Uranyl acetate (2% w/v) was added to the grid for 2 minutes and subsequently washed three times with one millilitre of distilled water. Grids were left overnight over filter paper to dry them. Images were taken using a JEOL 2000 FXII transmission electron microscope (Jeol Ltd., Tokyo, Japan).

2.7.2. Atomic force microscopy (AFM)

AFM samples were prepared using silicon wafer shards, adding the insulin glulisine NPs solution previously diluted in distilled water (1:100). Surface topography was analysed using a Park Systems (XE-100) under ambient conditions. Scans were performed in non-contact mode with high resolution, silicon micro-cantilever tips. Topographic images were recorded at a resonance frequency of 270-330 kHz.

2.8. Quantification of insulin association efficiency

Following nanoparticle preparation, non-associated insulin was separated from the NPs using a combined filtration-centrifugation approach. A total volume of 400 µl of sample was placed in the sample reservoir of the centrifugal filters (Amicon Ultracel® MWCO 30 kDa Millipore) and centrifuged for 25 min (4650 g, 20 °C). After centrifugation, the solution in

the acceptor compartment was examined to quantify non-associated insulin by high pressure liquid chromatography (HPLC) (*Section 2.11).* The association efficiency and the peptide loading of the NP formulation were calculated using equations 1 and 2, respectively.

$$\textbf{\textit{Association efficiency}}\ (\text{AE}\,\%) = \frac{\text{Insulin in the isolated nanoparticles}}{\text{Total Insulin}} \times 100 \qquad \textbf{Equation 1}$$

$$\textbf{\textit{Peptide loading}}\ (\%) = \frac{\textbf{Total insulin added} \times \textbf{AE}}{\textbf{Total weight of NPs}}\ \textbf{x 100} \qquad \textbf{Equation 2}$$

2.9. Disruption of the NP structure

The extraction of the insulin from the isolated nanoparticles by the complete disruption of the nanocarrier was performed by digestion of the particles with a mixture of acetonitrile and Triton®-X-100 (1:1:1 volume ratio NP: ACN: Triton®-X-100), followed by vortexing for 30 seconds. The resulting sample was diluted 1:1 with the HPLC mobile phase. The insulin concentration was determined by HPLC (*Section 2.11).*

2.10. Yield of production

The yield of the production (*w/w*) of insulin glulisine NPs was determined following freeze-drying of the isolated nanoparticles (Virtis Advantage Pro™, USA). Vials were weighed before the process (with and without the nanoparticle formulation solution) and after the freeze-drying procedure, and the yield of production was calculated as a percentage related to the theoretical nanoparticle concentration (Equation 3).

$$\textbf{\textit{Yield}}\ (\%) = \frac{\textit{NP weight before the F.D process}}{\textit{Nanoparticles weight after the F.D process}}\ x\ 100 \qquad \textbf{Equation 3}$$

- *NP weight before the F.D. process: weight of the vial after the addition of the NP solution - weight of the empty vial*
- *NP weight after the F.D. process: weight of the vial after the F.D process- weight of the empty vial*

2.11. Insulin concentration quantification by reverse phase HPLC

Insulin concentrations from *in vitro* samples were determined by reverse phase HPLC using an Agilent 1200 HPLC apparatus. Samples (10 µL) were injected into a LiChroCART 125-4 column (Superspher 100 RP-18 9125 mmx 4 mm i.d) packed with a matrix of octadecylsilane-coated silica beads of 100 Å pore size. The HPLC method utilized for the insulin glulisine quantification was kindly provided by Sanofi-Aventis. Briefly, 0.1 M of phosphoric acid and 0.3 M of sodium perchlorate were dissolved in 1.6 L of water for chromatography. The pH was adjusted to 2.3 with trimethylamine and volume was increased to 2 L. The buffer solution was diluted with acetonitrile to obtain the mobile phase A and B (93:7 and 43:57 volumes of buffer: acetonitrile, respectively). After preparation, the pH of both phases was adjusted to 2.3 with phosphoric acid. Mobile phases A and B were mixed in a ratio A: B = 44:56 to obtain an isocratic gradient. Column temperature was set at 35 ˚C and the flow of the mobile phase was adjusted to 1 mL/min. Insulin quantification was performed using a calibration curve of the peak area versus

concentration of the insulin glulisine (0.5 to 0.0078125 µg/µL). Linearity was observed in this concentration range, with a correlation coefficient above 0.99.

2.12. Biorelevant media preparation

The stability of insulin glulisine NPs was evaluated in simulated intestinal fluid (SIF), SIF supplemented with pancreatin (1 % w/v, 4 Unite States Pharmacopeia (USP) specifications), fasted state simulated intestinal fluid (FaSSIF-V2) and Hanks balanced salt solution (HBSS). The stability of the nanocomplexes was not assessed in gastric fluids due to the availability of gastro-resistant capsules which would enable the nanoparticles to bypass the stomach and be released in the intestine. The preparation of the two biorelevant media was performed as follows:

2.12.1. Simulated intestinal fluid (SIF)

NaOH (0.3 g) was added and vigorously stirred into a solution of 3.4 g of KH_2PO_4 in distilled water, the volume was adjusted to 250 mL with distilled water and the pH adjusted to 6.8 with either HCL or NaOH. After the pH adjustment, the volume was increased to 500 mL with distilled water (16).

2.12.2. SIF supplemented with pancreatin 1 % (w/v)

Supplemented SIF was prepared following the protocol described in previous studies by *Guo et al*. (17): 0.68 g of KH_2PO_4 were dissolved in 25 mL of deionized water. 19 mL of NaOH 0.2 and 40 mL of distilled water were added to the solution, in addition to 1 g of pancreatin (4 USP). The pH was adjusted with NaOH 0.2 N to pH 7.5 ± 0.1 and the volume to 100 mL with deionized water. Aliquots of 2 mL were centrifuged at 18,620 g for 30 min. Following centrifugation, 1 mL of the supernatant from each vial was carefully collected and use for the experiments.

2.12.3. Fasted state simulated intestinal fluid (FaSSIF-V2)

In the case of FaSSIF-V2, 3.9 g of NaOH, 2.22 g maleic acid and 4.0 g of NaCl were dissolved in 1 L of distilled water. The pH of the solution was adjusted to 6.5 (FaSSIF-V2 blank). Sodium taurocholate (1.61 g) was dissolved in 500 mL of this blank FaSSIF-V2. Concurrently, 0.15 g of lecithin were dissolved in a minimum volume methylene chloride. The methylene chloride solution was added to the 500 mL of this blank FaSSIF-V2, yielding a white emulsion. The methylene chloride is then eliminated under vacuum at 40˚C using a rotary evaporator and the volume is adjusted to 1 L with blank buffer.

2.12.4. Small intestinal fluid collection from pigs

Five male landrace pigs (15–20 kg, mean 17.5 kg) were sourced locally and housed at the University's Biological Services Unit (BSU). The study was carried out under licences issued by the Department of Health, Ireland, as directed by the Cruelty to Animals Act, Ireland and EU Statutory Instruments (project licence B100/2877). Local University ethical committee approval was also obtained. Pigs were fasted for 16 h before experiments. Animals were euthanized by intravenous injection of pentobarbital sodium followed by potassium chloride

(KCl). The peritoneal cavity was exposed via midline incision and the stomach and small intestine were located and isolated. Occluding ligatures were applied to the distal and proximal ends of the small intestine. The luminal content was removed and placed in 50 ml sterilised collection tubes. The luminal extracts were homogenized using a T25 Ultra-Turrax® homogenizer probe (5 min, 200 rpm). After the treatment, 0.2 mL of NaCl 0.125 M were added to 1.8 mL of the homogenised fluids. Samples were centrifuged to remove the solid components of the luminal content (15 min, 21380 g, 4˚C). After the isolation process, a pellet was obtained, and 1.5 mL of supernatant were collected and frozen at -80 ˚C (18).

2.13. Colloidal stability in simulated intestinal fluids

150 µL of the isolated insulin glulisine NPs were diluted with 850 µL of the different biorelevant media, and samples were placed under mild shaking (300 rpm, RT Thermomixer confort, thermomixer R. Eppendorf. Sigma-Aldrich) at 37˚C. The stability was evaluated at different time points using the DLS technique by fixing the attenuator value and monitoring changes in size, PdI and count rate of the prototypes over 4 hours.

2.14. Protein stability in simulated intestinal fluids containing enzymes

2.14.1. Validation of the technique

Prior to the experiment, the supplemented SIF (1 % w/v) was diluted up to 1:5 due to the high background signal of the media. Two different controls were run prior to the evaluation of the different nanoparticle formulations: i) an insulin solution (0.5 µg/µL) with supplemented SIF in a volume ratio 1:1 and ii) an insulin solution (0.5 µg/µL) with aprotinin (0.2 µg/µL) and supplemented SIF in a volume ratio 0.5:0.5:1 of insulin: aprotinin: supplemented SIF.

2.14.2. Proteolysis assay

The protection conferred to the insulin glulisine after inclusion into the nanoparticle formulation was evaluated upon incubation with a solution of supplemented SIF with pancreatin (4 USP, 1% w/v, 1:5 dilution) and separately with a solution of pig enzymes in a ratio volume of 1:1. In both cases, a control was performed with the same initial concentration of the protein used for preparation of the formulations. Circular dichroism profiles were recorded as previously explained in *Section 2.2.*, fixing the temperature at 37°C. The background due to the different components of the formulation and the media was recorded and subtracted from the NPs profiles. In the case of the solution of the naked protein, the corresponding background of the proteolytic media was recorded and subtracted.

2.15. Evaluation of the insulin bioactivity in human hepatocellular carcinoma cells (Hep G2)

Insulin glulisine NPs were prepared following the protocol described in *Section 2.5*. Nanoparticles were isolated using the combined filtration-centrifugation method previously described in *Section 2.8*. To release the insulin from the nanoparticle structure, the formulation was digested as previously described in *Section 2.9*. Hep G2 cells (passage 3 to 20) were extracted from a human liver carcinoma and are enriched in insulin receptor

expression (19). The cells were cultivated in EMEM (1 g glucose/L), supplemented with 10 % FBS, 1% non-essential amino acids, 1% penicillin (100 U/mL), 1% streptomycin (100 µg/mL) and 2 mM L-Glutamine (37°C, 95 % of relative humidity and 5 % CO_2).

Insulin bioactivity was evaluated in transfected Hep G2 cells by measuring the luciferase expression triggered by the transcription of a plasmid (*pSynSRE-T-luc;* Addgene, Cambridge USA) containing DNA Response Elements for Sterol regulatory element-binding proteins (SREBPs) (20). This promoter responds to insulin in a concentration-dependent manner, leading to increased production of fluorescent luciferase (21, 22). pSynSRE-T-luc contains the −324 to −225 bp fragment of the hamster HMG-CoA synthase promoter containing the SREBPs elements upstream of the minimal HMG-CoA synthase TATA box (−28 to +39). As a control to ensure a specific response to insulin glulisine, a plasmid with four mutated nucleotides at the same DNA response elements in the same promoter were transfected in parallel and tested for insulin activity (*pSynSRE-mut-T-luc*) (23, 24). Insulin regulates the HMG-CoA synthase expression through those SREBPs in human cells, this is the mechanism of action supressed in the mutated promoter (25).

Hep G2 were seeded 24 hours prior to the assay in 96-well MW48 multiwell plates (Costar, Thermo NY USA) at a density of 2.4x 10^3 cells per well. The wells were coated with 40 µL/well of freshly prepared Type I collagen solution (100 µg/mL) in PBS (stock solution of 4 mg/mL; SIGMA, St Louis MO, USA). After 24 hours, transfection studies were performed by adding 25 µL of the transfection mix of DNA plasmid (85 ng of the corresponding promoter (*pSynSRE-T-luc or pSynSRE-mut-T-luc)* + 35 ng of pRVS-βgal plasmid per well), Viafect transfection reagent (1.5 µL/well) and EMEM (23.5 µL/well) for 20 minutes. Upon 6 hours incubation, the wells were washed three times with warmed PBS and 400 µL of culture deprivation media containing the different samples (n=6/8) were added for 4 hours. The deprivation media presents the same composition as the growth medium with only 0.5% FBS and supplemented with 2 mM of metformin. The luciferase expression levels were measured upon contact with different concentrations of i) insulin glulisine NPs, ii) insulin glulisine solution, iii) a mixture of the different components of the formulation and insulin glulisine, iv) the insulin glulisine NPs digested prior to the assay and v) the mixture of the different components of the formulation digested prior to the assay. After 20 hours, wells were washed three times with PBS followed by the addition of 40 µL of PassiveLysis Buffer per well (Promega, Madison USA) for 20 minutes. Lysates were collected and frozen at -20º C. Luciferase activity was measured in a Mithras microplate reader (LB940, Berthold, Bad Wildbad Germany) using 15 µL of lysate as previously described (26). Experiments performed in triplicate and the fluorescent values of the samples were expressed as ΔLuc (increment of the Luciferase activity/β-Galactosidase).

Statistical analysis was performed assessing the normality of the data applying a Kolmogorov-Smirnov test. If the data followed a normal distribution, a t-test was applied. If the data did not follow a normal distribution, the Mann-Whitney test was selected for the analysis. Differences were considered statistically significant if $p < 0.05$.

2.16. In situ intra-intestinal instillations in rats

Animal experimental procedures were performed in compliance with the Health Products Regulatory Authority (HPRA) under licence AE18982/P036 and the University College Dublin Animal Research Ethics Committee (AREC 13-40-Brayden). Male Wistar rats weighing 294–353 g were randomly assigned to the different groups. Animals were housed under

controlled conditions of temperature and humidity with a 12:12 h light/dark cycle. Rats received filtered water and standard laboratory chow *ad lib* and were fasted 16–20 h prior to the procedure with free access to water. Animals were anaesthetised using isoflurane (Iso-Vet, 1000 mg/g isoflurane liquid for inhalation, Piramal Healthcare, UK) at a flow rate of 5 L/min mixed with 4 L/min O_2 in an induction box. Once under anaesthesia, animals were transferred to a delivery mask and the rate was reduced to 4 L/min mixed with 2 L/min O_2. Anaesthesia was maintained with the same gas at 2-3 L/min mixed with 2 L/min O_2 using an anaesthesia vaporising unit (Blease Medical Equipment Ltd., UK). Rats were euthanized at the end of experiments by overdosing with 0.5 ml Euthatal™ (Merial Animal Health Ltd., UK).

The pharmacokinetic (PK) and pharmacodynamics (PD) studies were performed using an *in situ* instillation method as previously described by Aguirre *et al.* (27). This administration route, which bypasses the stomach, was selected due to the availability of gastro-resistant capsules which would enable the nanoparticles to bypass the stomach and be released in the intestine. Moreover, the instillation method is an initial screening tool in that it offers a best-case scenario for presenting the insulin-entrapped construct to the intestinal epithelium in high concentrations, ahead of further investment in formulation approaches. The jejunum was exposed after a midline laparotomy. Approximately 5-7 cm jejunum was isolated by tying the extremities up with size 4 braided silk suture (Mersilk®, Ethicon Ltd., UK). Insulin glulisine solution (50 IU/kg), insulin glulisine NPs (50 IU/kg) and PBS (negative control), were instilled using a 30G needle. To calculate relative bioavaiability (% F), one treatment group was administered insulin solution (1 IU/kg) subcutaneously. Blood samples were withdrawn from the tail vein to monitor the change in the glucose levels following administration of insulin glulisine NPs, insulin solution, and PBS. In parallel, blood samples totalling ~350 µL were taken from anaesthetised animals via retroorbital venepuncture using a glass capillary tube of 1.35 mm internal diameter cut in two (75 mm total length) at pre-determined intervals. Samples were kept on ice before being centrifuged (6500 g, 5 min, 4 °C). Blood glucose levels were measured using a hand-held glucometer (Accu-chek™ Aviva, Roche, Ireland) and were plotted against time. Plasma levels of insulin glulisine were measured by an exploratory LC-MS/MS method at Sanofi (Frankfurt). For calculation of mean concentrations, values below the lower limit of quantification (LLOQ = 0.1 ng/mL in plasma) were set to zero.

The PD response and the area above the curve (AAC) of blood glucose reduction were calculated and analysed using GraphPad Prism 7 software® and a two-way ANOVA with a *Bonferroni* post-test (28). Results were expressed as the mean ± SEM. A significant difference was considered to be present if $p < 0.05$. PK data was analysed using WinNonlin® 6.4 software using a non-compartmental model and linear trapezoidal interpolation calculation. Peak concentration (C_{max}), the time taken to reach C_{max} (T_{max}) and the $AUC_{0\text{-}4h}$ were calculated from the plasma concentration profiles. The mean relative oral versus the subcutaneous bioavailability were assessed based on $AUC_{0\text{-}4h}$ and corresponding doses.

2.18. Histology of the intestinal tissue samples

For histological evaluation, the isolated loops were immersed in 10 % (w/v) of formalin during 24 h and embedded in paraffin wax. 5 µm sections were cut on a microtome (Leitz 1512; GMI, USA), mounted on adhesive coated slides, and stained with haematoxylin and eosin (H&E) or Alcian blue. The different sections were visualised under a light microscope (Nikon Labphoto; Nikon, Japan) and images were taken with high-resolution camera (Micropublisher 3.3 RTV; Q Imaging, Canada) and Image-Pro® Plus version 6.3 acquisition software (Media Cybernetics Inc., USA).

RESULTS AND DISCUSSION

3.1. Pre-formulation studies with insulin glulisine: influence of pH on structure

The stability and the physicochemical properties of proteins are influenced by many parameters such as the protein isoelectric point, temperature, and the pH of the protein solution (29). Due to the amphoteric nature of proteins, these macromolecules form complexes with positively- and negatively charged compounds. Insulin monomers present 6 amino acid residues which are able to bind positively-charged materials and 10 amino acid residues capable of binding negatively-charged materials (30). In order to estimate the charge of insulin glulisine and identify the optimum conditions to develop a nanocomplex with the click propyl-amine CD, an estimation of the net charge of the protein at different pHs was performed using the *Protein Calculator v3.4* (31).

Figure 1A shows insulin glulisine net charge over the pH range 1-12, identifying the contribution of each chain to the final charge of the protein. In addition, an estimation of the isoelectric point and the molecular weight of the protein was performed. As observed in **Figure 1B**, the results obtained for the isoelectric point and the molecular weight via the software are very close to the values provided by the supplier (5.0 and 5829 versus 4.8 and 5823 g/mol, respectively).

To complete the characterization of insulin glulisine, circular dichroism profiles were recorded over a range of pH and the CDNN software was utilized to estimate insulin secondary structure in the far-UV region (180-260 nm). These CDNN estimations are based on the comparison between the CD spectras of the test protein to reference profiles of known proteins structures. The approximate contribution of the different protein components (α-helix, β-sheet, β-turn and random coil) to the overall structure (*Circular dichroism spectra deconvolution)* was estimated using the CDNN software. Only minor conformational changes were detected at the different pHs, with the exception of pH 5, where the α- helix values decreased compared to other profiles (**Figure 1D**). These changes in the insulin conformation could be explained by the isoelectric point of the protein, which is close to 5, where the protein may show a different structure relative to other pHs. These results, together with the cationic nature of the click propyl-amine CD, indicate that complex formation will be favoured at pH above 4.8. As it is envisaged that the final dosage would be a gastro resistant capsule, which would only release in the small intestine, a pH of 6.6 was selected for further development of the nanoparticle formulation.

A

pH	B Chain [pI = 6.48] IAMW: 3444.96 g/mol	A Chain [pI= 3.53] IAMW: 2383.70 g/mol	Overall Average
1	5	1	6
1.5	5	1	6
2	4.9	0.9	5.8
2.5	4.8	0.8	5.6
3	4.4	0.5	4.9
3.5	3.9	0.1	4
4	3.3	-0.5	2.8
4.5	2.3	-1.1	1.2
5	1.6	-1.6	0
5.5	1	-1.9	-0.9
6	0.6	-2	-1.4
6.5	0	-2.1	-2.1
7	-0.7	-2.2	-2.9
7.5	-1.2	-2.6	-3.8
8	-1.9	-3.5	-5.4
8.5	-2.8	-4.8	-7.6
9	-3.7	-6.1	-9.8
9.5	-4.5	-7.1	-11.6
10	-5.4	-7.9	-13.3
10.5	-6.3	-8.5	-14.8
11	-6.8	-8.8	-15.6
11.5	-7.1	-8.9	-16
12	-7.5	-9	-16.5

B

Isoelectric point (pI)		Molecular weight (MW; g/mol)	
Supplier pI	Calculated pI	Supplier MW	Calculated MW
4.8	5.0	5823	5828.66

C

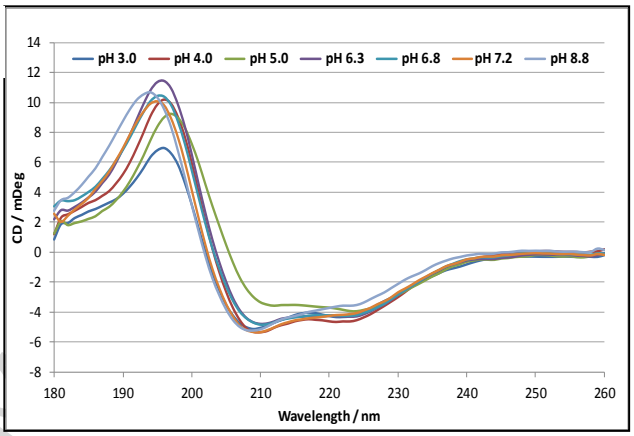

D

CDNN (180-260 nm)	pH 3.0	4.0	5.0	6.3	6.8	7.2	8.8
% α-helix	32.9	37.4	31.1	38.4	37.7	37.8	37.9
% β-sheet	18	13.7	13.7	12.9	13.3	13.5	13.5
% β-turn	17.3	15.9	15.9	15.4	15.7	16.1	16.2
% Random coil	31.8	32.7	32.7	34.3	33.4	30.1	28.9

Figure 1: (A) Charge of the different chains and overall charge of insulin glulisine at different pH values as predicted by *Protein Calculator v3.4*. **(B)** Isoelectric point and molecular weight values obtained with the protein calculator v3.4 and provided by the supplier. (*IAMW: Isotopically Averaged Molecular Weight; pI: isoelectric point of the protein).* **(C)** Circular dichroism profiles of insulin glulisine (0.5 µg/µL) over the pH range 3-8.8. **(D)** CDNN deconvolution of insulin glulisine profiles (0.5 µg/µl) over the pH range 3-8.8.

3.2. Evaluation of the binding properties of the amphiphilic cationic CD and optimization of insulin glulisine NPs prepared using the layer-by-layer approach

A range of nanocomplexes were prepared between the CD and insulin glulisine (molar ratio 1:3; 1:7 and 1:14 insulin: CD) as described in *Section 2.3*. The binding properties of the CD following NP synthesis at pH 6.5 were analysed by PAGE electrophoresis. The results indicate a high degree of complexation at the different ratios tested: the complexed insulin

was estimated to be 93, 95 and 100 % for molar ratio 1:3, 1:7 and 1:14, respectively (**Figure 2A).**

In spite of these promising results, the NPs displayed poor stability upon contact with simulated intestinal fluids (data not shown). In order to enhance the stability particularly in the presence of proteolytic enzymes, two components were added to the primary complex: a negatively-charged polymer, dextran sulphate, and a PEGylated phospholipid, mPEG-DSPE 2000. The molar ratio of 1:4 (insulin glulisine: cyclodextrin) when combined with dextran sulphate gave the best stability profiles which maintained a nanometric size for 3 hours upon contact with simulated intestinal fluids **(Figure 2B)**. However, the increase in the count rate detected over time may indicate that the particles are undergoing a disintegration process. To further improve the profile, mPEG-DSPE 2000 was added by post-insertion into the CD layer before addition of dextran sulphate. The optimum molar ratio of the four components in terms of stability profile was identified in 1:4:4:3 of insulin glulisine: cyclodextrin: mDSPE PEG 2000: dextran sulphate (**Figure 2C**). Photon correlation spectroscopy analysis showed a population of NP with a size of 103 ± 5 nm, substantially smaller than previous results reported for other cyclodextrin-based nanoparticles containing a protein cargo (32), with a negative zeta potential -30 ± 2 similar to that previously reported for cyclodextrin-based protein nanocarriers (33) and a relatively low polydispersity index of 0.272.

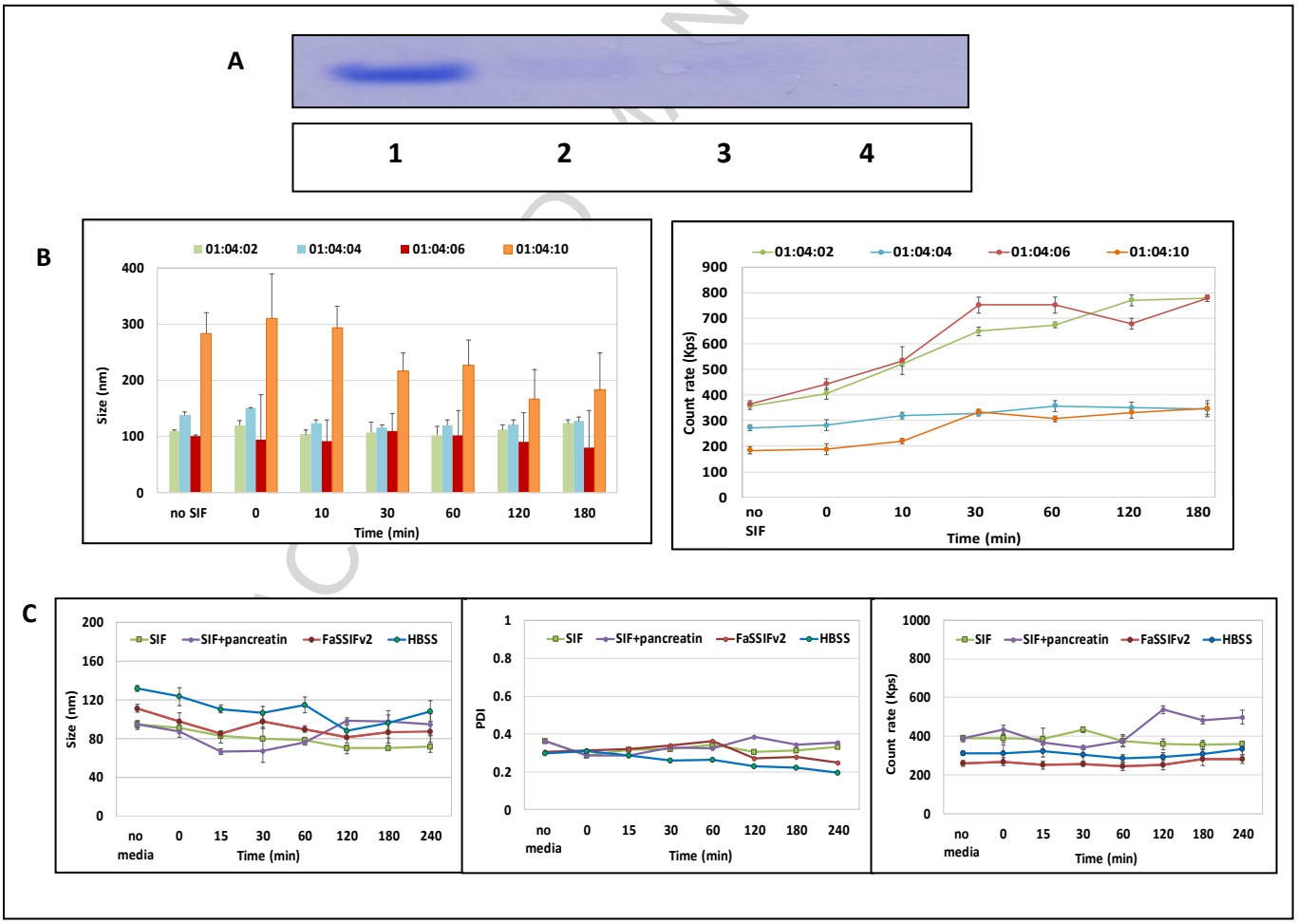

Figure 2: **(A)** Native-PAGE gel of insulin glulisine and insulin glulisine: CD nanocomplexes at different molar ratios. From left to right, insulin glulisine 10 µg (1); insulin glulisine: CD molar ratio 3 (2); insulin glulisine: CD molar ratio 7 (3); insulin glulisine: CD molar ratio 14 (4). **(B)** Mean particle size

(left) and count rate (right) of different nanoparticle formulations incorporating different ratios of dextran sulphate (stability in SIF for 3 hours at 37˚C n=3 +/- S.D.). **(C)** From left to right: Mean particle size, PDI and count rate of insulin glulisine NPs molar ratio 1:4:4:3 of insulin glulisine: CD : mDSPE PEG 2000: dextran sulphate upon contact with different media (SIF, SIF + pancreatin 1 % (w/v), FaSSIF-V2 and HBSS) for 4 hours at 37˚C (n=3 +/- S.D.).

3.3. Production yield, encapsulation efficiency and morphological evaluation of the insulin glulisine NPs: Transmission electron microscopy (TEM) and Atomic Force Microscopy (AFM)

The production yield for the optimised formulation was estimated to be 97.2 ± 6.4 %. In addition, the loading and the AE (Association Efficiency) for insulin glulisine were quantified after the isolation of the particles. Following the filtration-centrifugation approach, non-associated insulin was estimated in 24.7 ± 4.5 % and the direct quantification confirmed the results achieved with the indirect method: the average AE was established in 71.4 ± 3.4 % for a peptide loading of 10.2%. This AE results are superior to those previously reported for β-cyclodextrin based nanosystems including PEG2000 molecules (34) and PEG molecules of higher molecular weights (35). After the isolation, the formulation was able to keep its nanometric size and negative zeta potential, improving its PDI index after the isolation process (**Figure 3A**).

With respect to the NP morphology, TEM images showed a population with a spherical shape (**Figure 3B**). The hydrodynamic diameter as measured by DLS tended to be greater than the size observed by TEM analysis due to the dehydration process required for TEM samples. The AFM images showed a homogeneous spherical population of particles where the main population of particles had an average size of 100 nm, in agreement with DLS results (**Figure 3C**).

A

	Size (nm)	PdI	Zeta potential (mV)	Association efficiency (%)	Peptide loading (%)	Yield of production (%)
Before isolation	103 ± 5	0.278	-30 ± 2	…	….	….
After isolation	109 ± 9	0.273	-25 ± 3	71.4 ± 3.37	10.2	97.20 ± 6.35

B

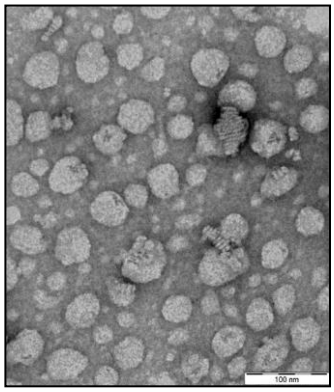

C

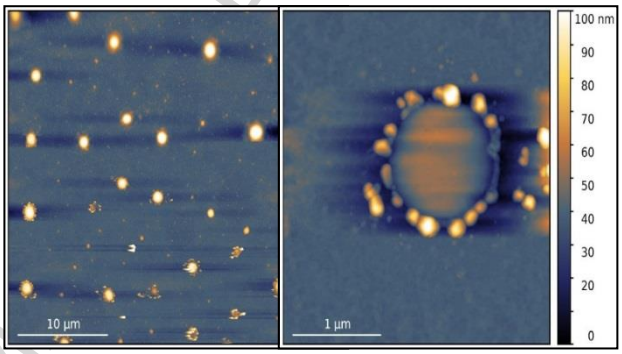

Figure 3: (A) Physicochemical properties of insulin glulisine NPs (insulin glulisine: cyclodextrin: mDSPE PEG 2000: dextran sulphate molar ratio 1:4:4:3) before and after isolation (n=3 +/- S.D.). (B) TEM image of insulin glulisine NPs prepared using uranyl acetate 2% (w/v) x200k. (C) AFM images of insulin glulisine NPs.

3.4. Insulin stability in the nanoparticle formulation following exposure to SIF containing enzymes

Circular dichroism was used to monitor the secondary structure of insulin glulisine following inclusion into the nanoparticle formulation compared to a solution of insulin glulisine. Results show the structural profile of the insulin glulisine was maintained after the formulation process. The CDNN analysis shows no major changes in the different structural components relative to the insulin control (**Figure 4 A&B**).

On incubation with proteolytic enzymes, insulin glulisine was rapidly degraded (**Figure 4C** right & **4D**). The incorporation of the enzyme inhibitor, aprotinin, protected against this degradation and maintained the structural integrity of the insulin solution (**Figure 4C left**). The CDNN analysis of the samples containing aprotinin (**Figure 4E**) indicates a reduction in insulin degradation over 90 min.

A

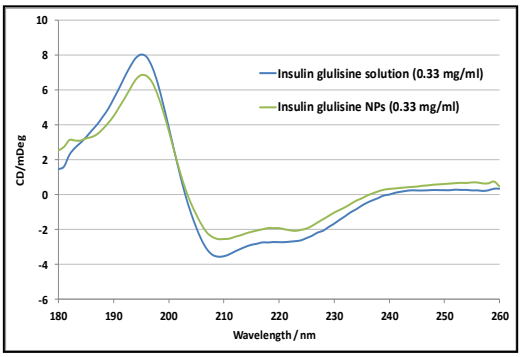

B

CDNN 180-260 nm	Insulin solution (0.33 mg/mL)	Insulin NPs (0.33 mg/mL)
α-helix	18.1	17.8
β-sheet	49.1	50.2
β-turn	20.8	20.9
Random coil	43.3	43.6

C

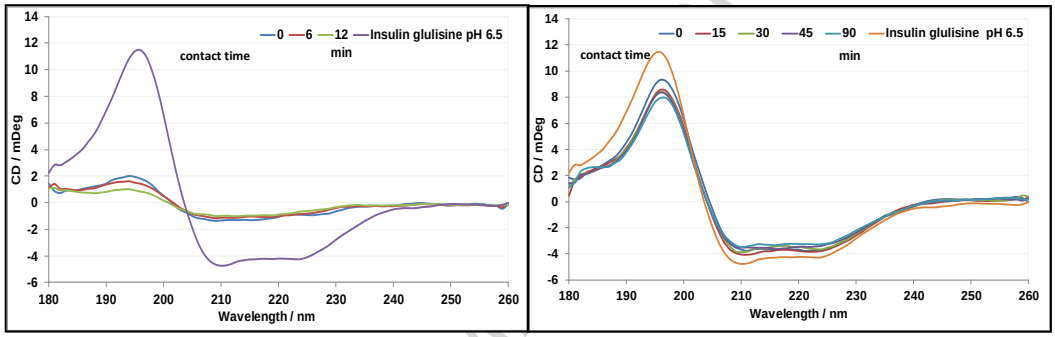

D

CDNN of Insulin glulisine 180-260 nm	Insulin glulisine pH 6.5	0 min	12 min
% α-helix	38.4	19.2	19.2
% β-sheet	12.9	43.7	43.7
% β-turn	15.4	20.1	20.1
% Random coil	34.3	44.7	44.7

E

CDNN Insulin glulisine :Aprotinin 180-260 nm	Insulin glulisine pH 6.3	0 min	15 min	30 min	45 min	90 min
% α-helix	38.4	36.1	35.8	34.9	34.5	33.7
% β-sheet	12.9	14.3	14.7	15.4	15.7	16.4
% β-turn	15.4	15.9	16.10	16.3	16.3	16.5
% Random coil	34.3	35.2	33.7	34.4	34.7	35.1

Figure 4: (A) Circular dichroism spectra of insulin glulisine NPs and the control insulin glulisine solution (n=3; 0.33 µg/µL). **(B)** CDNN deconvolution of the control insulin glulisine solution (0.33 µg/µL) and insulin glulisine after formulation. **(C)** Proteolysis studies of insulin glulisine solution control (right) and insulin glulisine plus aprotinin (left), with supplemented SIF (n=3). **(D)** CDNN of insulin glulisine (0.5 µg/µL) before and upon contact a solution of the supplemented SIF at different time points **(E)** CDNN of insulin glulisine (0.5 µg/µL) with aprotinin (0.2 µg/µL) before and upon contact with a solution of supplemented SIF 1 % (n=3).

Based on the results described above (**Figure 4**), circular dichroism was used to monitor the stability of insulin glulisine in the NPs following exposure to the proteolytic media. As previously reported, free insulin glulisine solution was completely degraded upon contact with the biorelevant media (**Figure 4A**), in contrast, insulin glulisine NPs are able to protect the insulin from the degradation, improving substantially the profile achieved relative to free insulin (**Figure 5A**). In both cases, the contribution of the β-sheet increases when the samples are in contact with the proteolytic enzymes, but in the case of the insulin glulisine NPs the degradation is delayed due to the protective effect of the formulation (**Table 5B**). In parallel, the contribution of the α-helix decreases substantially over time, and the β-turn contribution increases in both samples.

The major difference detected between the two CDNN analyses is the change in the contribution of the random coil to the protein structure: the percentage of this protein section increases in the case of the insulin glulisine solution **(Figure 4B)**, whereas in the case of the nanoparticle formulation the random coil contribution decreases over time **(Figure 5B)**. According to the results previously obtained in a temperature study perform with the insulin glulisine solution, the random coil percentage increases at high temperatures (75˚C), when the insulin is unable to maintain its secondary structure (data not shown). Therefore, these results suggest that the formulation protects insulin from degradation by proteolytic enzymes to some extent.

A similar proteolysis study was repeated in using pig intestinal fluids. The degradation rate of the insulin in the NP formulation was decreased compared to insulin glulisine solution (**Figure 5C**). The CDNN analysis showed the same degradation profile previously observed with the supplemented SIF: once insulin glulisine is in contact with the enzymes, the contribution of the α-helix to the overall structure decreases substantially over time compared to the values registered for the insulin glulisine solution at pH 6.5. The decrease in the α-helix was more pronounced in the case of insulin solution than the NP formulation. In addition, the β-sheet and the random coil contribution to the overall structure increased upon contact with proteolytic media; this increase was more evident for the insulin glulisine solution compared to the NP especially at later time points (**Table 5D**). The smaller decrease in the α-helix percentage and the smaller increase in both the β-sheet and the random coil contribution to the insulin structure suggest an insulin-protective role for the NP formulation.

A

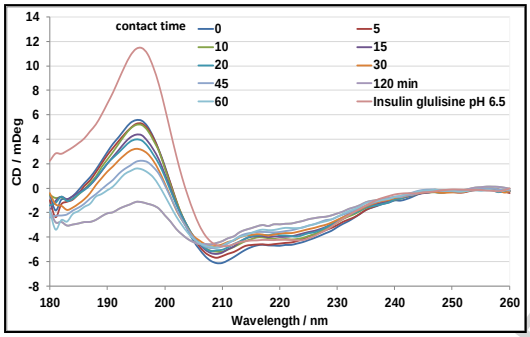

B

CDNN 180-260 nm	Insulin glulisine pH 6.5	0 min	20 min	30 min	45 min	60 min	120 min
% α-helix	38.4	30.9	29.4	28.0	24.4	23.7	20.4
% β-sheet	12.9	21.2	23.4	25.9	34.3	37.0	49.5
% β-turn	15.4	18.2	18.5	18.9	20.1	20.5	22.0
% Random coil	34.3	30.1	31.1	31.6	32.2	31.7	31.4

C

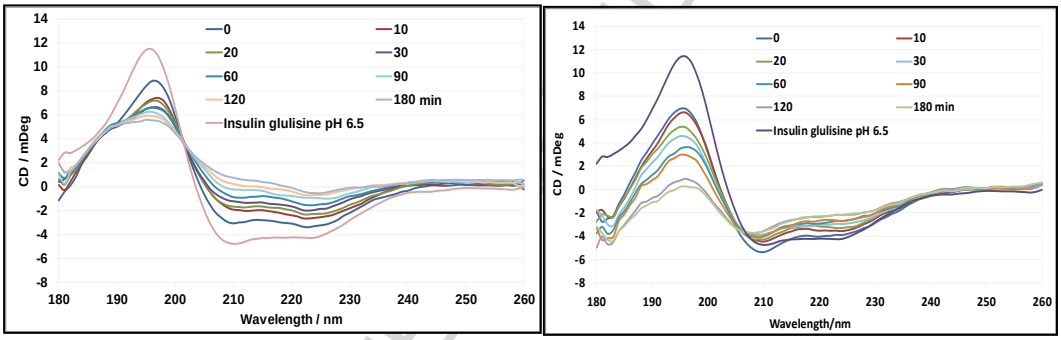

D

Insulin glulisine NPs CDNN 180-260 nm	Insulin glulisine pH 6.5	0 min	30 Min	60 min	90 min	120 min	180 min
% α-helix	38.4	30.9	28.0	24.2	23.7	21.5	20.4
% β-sheet	12.9	21.2	25.9	29.8	37.0	35.3	49.5
% β-turn	15.4	18.2	18.9	18.7	20.5	19.1	22.0
% Random coil	34.3	30.1	31.6	40.4	31.7	43.6	31.4
Insulin glulisine CDNN 180-260 nm	**Insulin glulisine pH 6.5**	**0 min**	**30 min**	**60 min**	**90 min**	**120 min**	**180 min**
% α-helix	38.4	24.1	22.7	21.8	21.5	19.1	18.4
% β-sheet	12.9	26.4	29.8	32.2	33.6	37.1	39.8
% β-turn	15.4	17.3	17.9	18.3	18.6	18.4	18.7
% Random coil	34.3	48.2	47.5	47.4	46.0	54.1	53.9

Figure 5: (A) Proteolysis studies of insulin glulisine NPs with supplemented SIF (n=3). **(B)** CDNN of insulin glulisine NPs with upon contact with supplemented SIF **(C)** Proteolysis studies of insulin glulisine control (left) and insulin glulisine NPs (right) with pig small intestinal fluids (n=3) . **(D)** CDNN of insulin glulisine NPs and insulin glulisine solution upon contact with a pig intestinal fluid.

3.5. Evaluation of the insulin glulisine bioactivity upon inclusion into the nanoparticle formulation.

In order to test the biological activity of insulin glulisine following incorporation into the NP formulation, a bioactivity assessment in Hep G2 cells was performed using different concentrations of insulin glulisine NPs. The luciferase expression levels were measured upon contact with different concentrations of i) insulin glulisine NPs, ii) a mixture of the different components of the formulation (blank NP) and insulin glulisine, iii) the insulin glulisine NPs digested prior to the assay (insulin glulisine NPs broken), and iv) a mixture of the different components of the formulation digested prior to the assay (blank NP blank).

As observed in **Figure 6A**, a solution with the different components of the formulation (blank NP) does not induce the expression of luciferase with *pSynSRE-T-luc* or *pSynSRE-mut-T-lu* at the different concentration tested (50 to 500 µU/mL). In contrast, insulin glulisine NPs were able to trigger the luciferase expression of pSynSRE-*T-luc* and not with the *pSynSRE-mut-T-lu* transcription factor. Statistical differences were found between the two groups in the range of concentrations tested (50 to 500 µU/mL, *pSynSRE-T-luc)*. In the case of the solution of the different components of the formulation plus a solution of insulin glulisine at two different concentrations (NP blank + insulin glulisine solution), similar levels of luciferase expression were observed for the two concentrations of insulin glulisine solution (75 to 125 µU/mL) (**Figure 6B**).

As observed in **Figure 6C**, no luciferase activity was registered upon contact with a solution of the different components of the formulation after its digestion at any of the concentrations tested (50 to 500 µU/mL). In contrast, when insulin was released from the NPs (insulin glulisine NP broken), increased luciferase expression was detected at 50 and 125 µU/mL compared to the data obtained with the intact undigested insulin glulisine NPs (2 fold higher approximately at 50 and 125 µU/mL of insulin concentration) (**Figure 6A**). No luciferase expression was observed at the highest NP insulin concentrations after the digestion process due to the requirement for high concentrations of Triton® -X-100 to digest the NPs, which also induce cell death. Overall, these results show that the formulation process for the NPs does not reduce bioactivity of entrapped insulin glulisine.

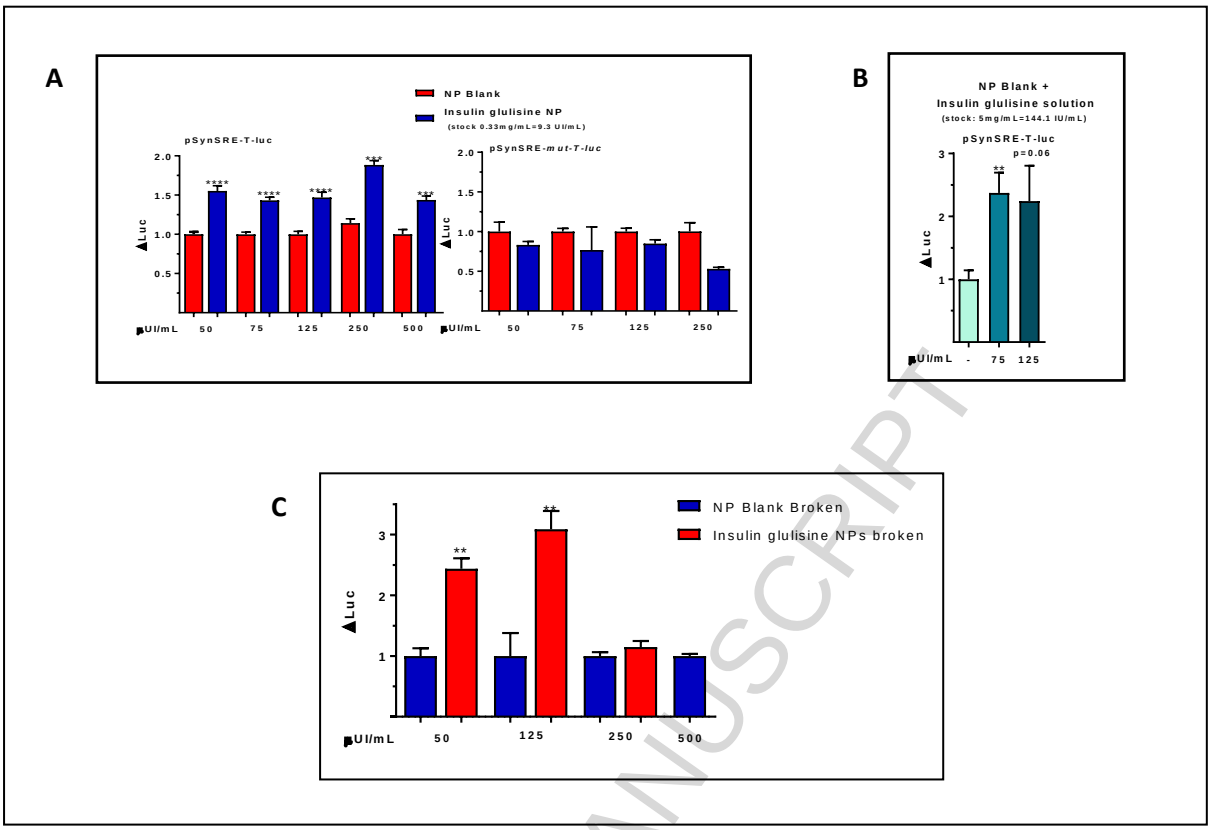

Figure 6: (A) Luciferase expression after the transcription of *pSynSRE-T-luc* and *pSynSRE-mut-T-luc* upon contact with a concentration range from 50 to 500 µU/mL of insulin glulisine NPs, a mixture of the different components of the formulation (NP blank) and a mixture of the different components of the formulation . **(B)** Luciferase expression after the transcription of *pSynSRE-T-luc* with a solution of the insulin glulisine and the different components of the formulations (NP blank + insulin glulisine solution) **(C)** Luciferase expression after the transcription of *pSynSRE-T-luc* upon contact with a concentration range from 50 to 500 µU/mL of insulin glulisine NPs after digestion (insulin glulisine NPs broken) and a solution of the different components of the formulation after its digestion (blank NP broken). Mean ± SEM of three independent determinations *(*p < 0.05; **p < 0.01; ***p < 0.005).*

3.6. In situ rat jejunal instillations: PD and PK analyses

3.6.1. Pharmacological response: reduction on the glucose blood levels

Insulin glulisine NPs were instilled to the jejunum of rats at a dose of 50 IU/kg. As observed in **Figure 7A**, neither PBS nor 50 IU/kg insulin solution induced a decrease in the blood glucose levels. In contrast, instillation of insulin glulisine NPs (50 IU/kg), led to a progressive reduction of glucose levels (≈50 % after 45 min relative to fasting levels), and the response was maintained up to 4 hours. Relative to the subcutaneous administration of insulin glulisine solution, the intestinal administration of the NPs achieved comparable overall reduction in the glucose levels (**Figure 7A**).

In order to compare the differences among the test groups, the pharmacological response was quantified utilising the area above the curve (AAC) at four different time points: 60; 120; 180 and 240 min. As shown in **Figure 7B**, the response from the insulin glulisine NPs (50 IU/kg; instillation versus the PBS was increased at all four time points compared. Compared to the

subcutaneous administration of insulin, the insulin glulisine NPs profile was similar but the response with the nanoparticle formulation was stronger at the later time points.

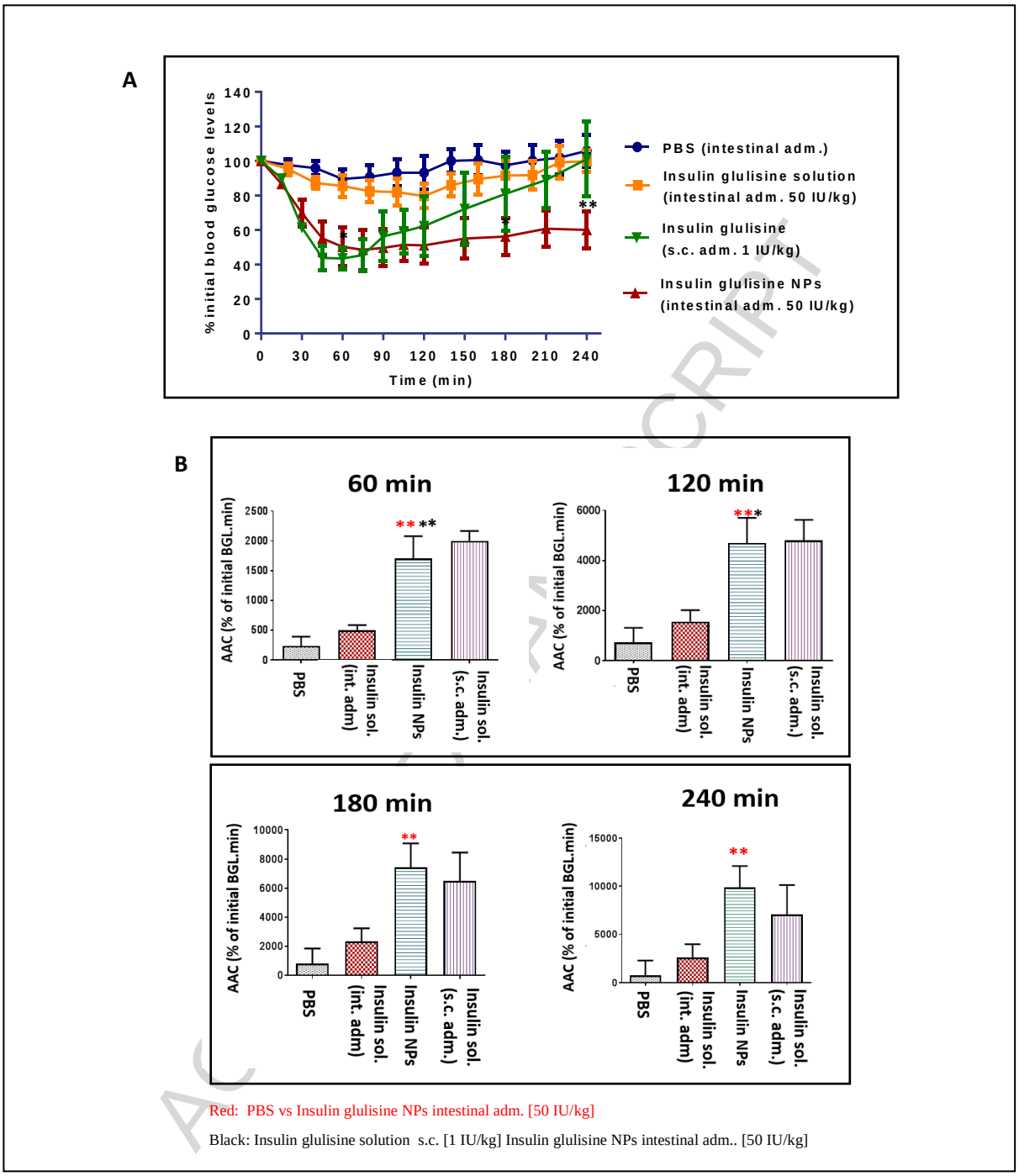

Figure 7: (A) Percentage of the initial blood glucose levels following exposure to insulin glulisine solution, insulin glulisine NPs, and PBS (n=6; and insulin glulisine solution (n=3; The error bars indicate the SEM *(*p < 0.05; **p < 0.01).* **(B)** Area above the curve at different time points NPs (n=6), and insulin glulisine solution (n=3)

3.6.2. PK analysis

Following intestinal administration of the NPs (50 IU/kg insulin) blood levels were detected and the profile is shown in **Figure 8 (A&B)** relative to that achieved following subcutaneous injection of insulin solution (1 IU/kg). Insulin glulisine NPs produced a delayed T_{max} compared to subcutaneous injection (0.875 *vs* 0.583 h) and a higher C_{max} (5.27 *vs* 2.8 nM/ml) (**Table 8C**). These results are broadly in agreement with the PD results: the AUC of the NP formulation (50 IU/kg) was three fold higher versus the insulin glulisine subcutaneous injection (1 IU/kg). The relative bioavailability (compared with the insulin solution administered subcutaneously) of insulin NPs was 5.5 % **(Figure 8D**) when administered intra-jejunally. A similar PD profile with a nanoparticle formulation using a chemically-modified cyclodextrin has been recently published by *Daimon et al*. In this study the effect of a novel polymeric carrier, based on β-cyclodextrin-grafted chitosan (BCC) with two different morphologies, on the intestinal absorption of insulin was investigated (36). Complexes prepared in an acetate buffer demonstrated a "molecular network structure". In contrast when a citrate buffer was used a nanoparticle formulation was identified. The *in vivo* studies showed that both complexes enhanced the intestinal absorption of insulin. A rapid absorption was achieved for the complex prepared in acetate buffer, whereas the nanoparticles from the citrate buffer produced a more sustained absorption profile. Additionally, the incorporation of the cell-penetrating peptide penetratin, either grafted to the BCC or added to a solution with the BCC, further enhanced the absorption profile of these formulations. The combination of a chemically-modified cyclodextrin and penetratin has previously produced similar results (37). In addition, similar results in terms of relative bioavailability have been previously described in the literature for other nanoparticle formulations such as solid lipid nanoparticles, which have shown enhanced oral relative bioavailability up to 4.9 % (38, 39). Furthermore, a polyelectrolyte complex prepared by coating a primary nanocomplex of insulin with trimethyl chitosan with doodecylamine-graft-gamma-polyglutamic acid (PGA-g-DA) displayed similar relative oral bioavailability results, reaching values of 5.9 % when compared to the subcutaneous control (40).

A

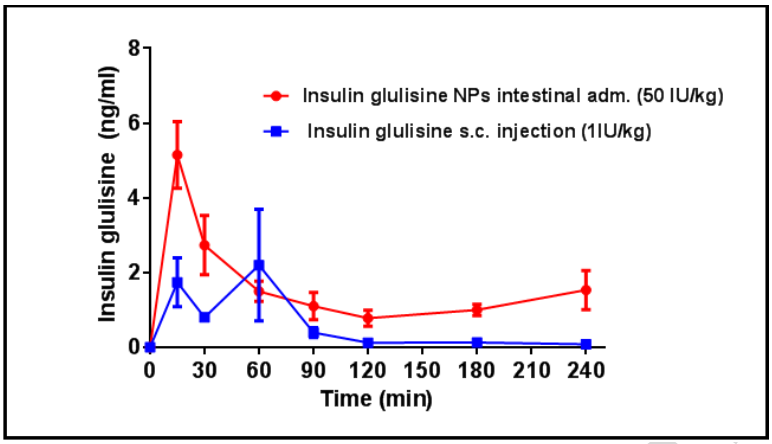

B

Treatment	Time (h)						
	0.25	0.50	1.0	1.5	2.0	3.0	4.0
	Concentration (ng/mL)						
S.c. injection of insulin glulisine (1 IU/kg)	1.74	0.80	2.20	0.39	0.12	0.13	0.08
Intra-intestinal adm insulin glulisine NPs (50 IU/kg)	5.15	2.73	1.50	1.32	0.78	1.00	1.53

C

	t_{max} (h)	C_{max} (ng/mL)	t_{last} (h)	AUC_{last} (h*ng/mL)
S.c. injection of insulin glulisine (1 IU/kg)	0.583	2.80	3.00	2.24
Intra-intestinal adm. insulin glulisine NPs (50 IU/kg)	0.875	5.27	4.00	6.10

D

	S.c. insulin glulisine solution (1 IU/kg) (h*ng/mL)	Intrajejunal adm. of insulin glulisine NPs (50 IU/kg) (h*ng/mL)	F_{rel} (%)
AUC_{last}	2.24	6.10	5.46

Figure 8: (A) Plasma insulin glulisine concentrations following intestinal administration of insulin glulisine NPs (n=6; 50 IU/kg) and insulin glulisine solution (n=3; 1 IU/kg) following subcutaneous administration. The error bars indicate the SEM *(*p < 0.05; **p < 0.01; ***p < 0.005).* **(B)** Mean plasma concentrations at different time points after the administration of insulin glulisine solution s.c. (1 IU/kg) and insulin glulisine NPs (n=6; 50 IU/kg; intestinal adm.). **(C)** Mean Plasma pharmacokinetic parameters after the administration of insulin glulisine solution (n=3; 1 IU/kg, s.c. and insulin glulisine NPs (n=6; 50 U/kg, intestinal adm.). **(D)** The relative bioavailability (F_{rel}) of the insulin glulisine NPs (n=6; 50 U/kg, intestinal adm.) compared with the insulin solution administered by s.c. (n=3; 1 IU/kg).

3.7. Assessment of the intestinal tissue integrity

To assess the integrity of the rat jejunal epithelium following exposure to the insulin glulisine NPs during instillations, the tissues were stained with haematoxylin and eosin (H&E) or Alcian blue. No significant damage to tissue was detected following exposure to the NP relative to the PBS or insulin solution controls over 240 min (**Figure 9**). Furthermore, the mucus barrier was maintained following insulin glulisine NPs treatment, as indicated by the Alcian blue staining.

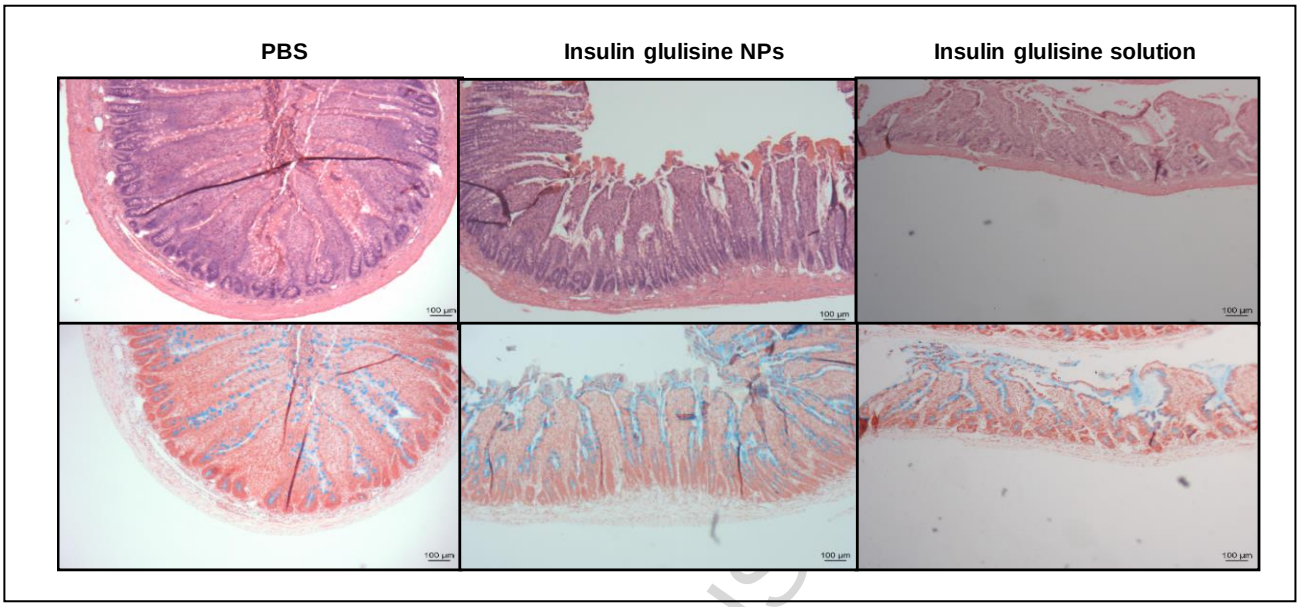

Figure 9: Intestinal histology at 4h following intra-intestinal instillation with PBS, insulin glulisine NPs and insulin glulisine solution (50IU/kg). H&E (top) and Alcian blue (4x) (bottom).

CONCLUSIONS

As previously reported with other other cationic (41) and amphipilic cyclodextrins (42), the click propyl-amine cyclodextrin was capable of complexing insulin glulisine to form particles in the nanometer size range (109 ± 9 nm) with a negative zeta potential (-25 ± 3 mV), a high loading (10.2 %) and a high AE (71.4 ± 3.37 %). The method of preparation produced a high yield, it was solvent free and did not cause any changes in the secondary structure of the protein. The resulting insulin glulisine NPs exhibited good colloidal stability upon contact with different biorelevant media (SIF, SIF supplemented with pancreatin 1 % (w/v), FaSSIF-V2 and HBSS) for up to 4 hours. Circular dichroism analyses showed that the NPs protected the insulin from intestinal enzymatic degradation.
Following *in vivo* intestinal instillation to rats, blood glucose reduction was detected indicating that the NP promoted absorption of insulin. NPs produced relative bioavailability of 5.5% compared to sub-cutaneous administration. Based on these initial results further development of NPs based on CDs for oral delivery of insulin and other peptides is warranted.

ACKNOWLEDGEMENTS

This work was supported by the European TRANS-INT Consortium, which received funding from the European Union's Seventh Framework Programme for research, technological development and demonstration under grant agreement No. 281035. The authors would like to thank Ms. M. Suarez-Fariña and Mr. M. Chenlo for the technical expertise in the cell bioactivity assay, Dr. M. Chronin for the assistance with the use of the circular dichroism equipment and Mr. Giuseppe Alessio for the atomic force microscopy analysis.

REFERENCES

1. Li X, Yu M, Fan W, Gan Y, Hovgaard L, Yang M. Orally active-targeted drug delivery systems for proteins and peptides. Expert Opinion on Drug Delivery. 2014;11(9):1435-47.
2. Li X, Guo S, Zhu C, Zhu Q, Gan Y, Rantanen J, et al. Intestinal mucosa permeability following oral insulin delivery using core shell corona nanolipoparticles. Biomaterials. 2013;34(37):9678-87.
3. Aronson R. The Role of Comfort and Discomfort in Insulin Therapy. Diabetes Technology & Therapeutics. 2012;14(8):741-7.
4. Owens DR. New horizons [mdash] alternative routes for insulin therapy. Nat Rev Drug Discov. 2002;1(7):529-40.
5. Barua S, Mitragotri S. Challenges associated with penetration of nanoparticles across cell and tissue barriers: A review of current status and future prospects. Nano Today. 2014;9(2):223-43.
6. Pinto Reis C, Neufeld RJ, Ribeiro AJ, Veiga F. Nanoencapsulation II. Biomedical applications and current status of peptide and protein nanoparticulate delivery systems. Nanomedicine: Nanotechnology, Biology and Medicine. 2006;2(2):53-65.
7. Niu Z, Conejos-Sánchez I, Griffin BT, O'Driscoll CM, Alonso MJ. Lipid-based nanocarriers for oral peptide delivery. Advanced Drug Delivery Reviews. 2016;106:337-54.
8. Becker RHA, Frick AD. Clinical Pharmacokinetics and Pharmacodynamics of Insulin Glulisine. Clinical Pharmacokinetics. 2008;47(1):7-20.
9. Bilensoy E, Hincal AA. Recent advances and future directions in amphiphilic cyclodextrin nanoparticles. Expert Opinion on Drug Delivery. 2009;6(11):1161-73.
10. O'Mahony AM, Ogier J, Desgranges S, Cryan JF, Darcy R, O'Driscoll CM. A click chemistry route to 2-functionalised PEGylated and cationic [small beta]-cyclodextrins: co-formulation opportunities for siRNA delivery. Organic & Biomolecular Chemistry. 2012;10(25):4954-60.
11. Garnock-Jones KP, Plosker GL. Insulin Glulisine. Drugs. 2009;69(8):1035-57.
12. O'Mahony AM, Godinho BMDC, Ogier J, Devocelle M, Darcy R, Cryan JF, et al. Click-Modified Cyclodextrins as Nonviral Vectors for Neuronal siRNA Delivery. ACS Chemical Neuroscience. 2012;3(10):744-52.
13. Fitzgerald KA, Malhotra M, Gooding M, Sallas F, Evans JC, Darcy R, et al. A novel, anisamide-targeted cyclodextrin nanoformulation for siRNA delivery to prostate cancer cells expressing the sigma-1 receptor. International Journal of Pharmaceutics. 2016;499(1–2):131-45.
14. Greenfield NJ. Using circular dichroism spectra to estimate protein secondary structure. Nature protocols. 2006;1(6):2876-90.
15. Chi Q, Huang K. Polyacrylamide Gel Electrophoresis of Insulin. Analytical Letters. 2007;40(1):95-102.
16. Niu Z, Tedesco E, Benetti F, Mabondzo A, Montagner IM, Marigo I, et al. Rational design of polyarginine nanocapsules intended to help peptides overcoming intestinal barriers. Journal of Controlled Release. 2017;263(Supplement C):4-17.
17. Guo J, O'Mahony AM, Cheng WP, O'Driscoll CM. Amphiphilic polyallylamine based polymeric micelles for siRNA delivery to the gastrointestinal tract: In vitro investigations. International Journal of Pharmaceutics. 2013;447(1–2):150-7.
18. Yao X, Bunt C, Cornish J, Quek S-Y, Wen J. Stability of Bovine Lactoferrin in Luminal Extracts and Mucosal Homogenates from Rat Intestine: A Prelude to Oral Absorption. Chemical Biology & Drug Design. 2014;84(6):676-84.
19. Uhlén M, Fagerberg L, Hallström BM, Lindskog C, Oksvold P, Mardinoglu A, et al. Tissue-based map of the human proteome. Science. 2015;347(6220).
20. Nadeau KJ, Leitner JW, Gurerich I, Draznin B. Insulin Regulation of Sterol Regulatory Element-binding Protein-1 Expression in L-6 Muscle Cells and 3T3 L1 Adipocytes. Journal of Biological Chemistry. 2004;279(33):34380-7.

21. Boizard M, Le Liepvre X, Lemarchand P, Foufelle F, Ferré P, Dugail I. Obesity-related Overexpression of Fatty-acid Synthase Gene in Adipose Tissue Involves Sterol Regulatory Element-binding Protein Transcription Factors. Journal of Biological Chemistry. 1998;273(44):29164-71.
22. Kakuma T, Lee Y, Higa M, Wang Z-w, Pan W, Shimomura I, et al. Leptin, troglitazone, and the expression of sterol regulatory element binding proteins in liver and pancreatic islets. Proceedings of the National Academy of Sciences. 2000;97(15):8536-41.
23. Dooley KA, Millinder S, Osborne TF. Sterol Regulation of 3-Hydroxy-3-Methylglutaryl-coenzyme A Synthase Gene through a Direct Interaction Between Sterol Regulatory Element Binding Protein and the Trimeric CCAAT-binding Factor/Nuclear Factor Y. Journal of Biological Chemistry. 1998;273(3):1349-56.
24. Smith JR, Osborne TF, Brown MS, Goldstein JL, Gil G. Multiple sterol regulatory elements in promoter for hamster 3-hydroxy-3-methylglutaryl-coenzyme A synthase. Journal of Biological Chemistry. 1988;263(34):18480-7.
25. Harris IR, Höppner H, Siefken W, Wittern K-P, Farrell AM. Regulation of HMG-CoA Synthase and HMG-CoA Reductase by Insulin and Epidermal Growth Factor in HaCaT Keratinocytes. Journal of Investigative Dermatology. 2000;114(1):83-7.
26. Garcia-Rendueles AR, Rodrigues JS, Garcia-Rendueles MER, Suarez-Fariña M, Perez-Romero S, Barreiro F, et al. Rewiring of the apoptotic TGF-β-SMAD/NFκB pathway through an oncogenic function of p27 in human papillary thyroid cancer. Oncogene. 2016;36:652.
27. Aguirre TAS, Rosa M, Coulter IS, Brayden DJ. In vitro and in vivo preclinical evaluation of a minisphere emulsion-based formulation (SmPill®) of salmon calcitonin. European Journal of Pharmaceutical Sciences. 2015;79:102-11.
28. Nielsen EJB, Yoshida S, Kamei N, Iwamae R, Khafagy E-S, Olsen J, et al. In vivo proof of concept of oral insulin delivery based on a co-administration strategy with the cell-penetrating peptide penetratin. Journal of Controlled Release. 2014;189:19-24.
29. Baheri M, Dayer MR. Temperature and pH Effects on Insulin Structure: A Molecular Dynamic Approach. Jentashapir J Health Res. 2016;7(4):e36931. Epub 2016-08-28.
30. Sarmento B, Ribeiro A, Veiga F, Ferreira D. Development and characterization of new insulin containing polysaccharide nanoparticles. Colloids and Surfaces B: Biointerfaces. 2006;53(2):193-202.
31. Altintoprak K, Seidenstücker A, Welle A, Eiben S, Atanasova P, Stitz N, et al. Peptide-equipped tobacco mosaic virus templates for selective and controllable biomineral deposition. Beilstein Journal of Nanotechnology. 2015;6:1399-412.
32. Gao H, Yang Y-w, Fan Y-g, Ma J-b. Conjugates of poly(dl-lactic acid) with ethylenediamino or diethylenetriamino bridged bis(β-cyclodextrin)s and their nanoparticles as protein delivery systems. Journal of Controlled Release. 2006;112(3):301-11.
33. Gao H, Wang YN, Fan YG, Ma JB. Synthesis of a biodegradable tadpole-shaped polymer via the coupling reaction of polylactide onto mono(6-(2-aminoethyl)amino-6-deoxy)-β-cyclodextrin and its properties as the new carrier of protein delivery system. Journal of Controlled Release. 2005;107(1):158-73.
34. Du X, Song N, Yang Y-W, Wu G, Ma J, Gao H. Reverse micelles based on [small beta]-cyclodextrin-incorporated amphiphilic polyurethane copolymers for protein delivery. Polymer Chemistry. 2014;5(18):5300-9.
35. Gu W-X, Zhu M, Song N, Du X, Yang Y-W, Gao H. Reverse micelles based on biocompatible [small beta]-cyclodextrin conjugated polyethylene glycol block polylactide for protein delivery. Journal of Materials Chemistry B. 2015;3(2):316-22.
36. Daimon Y, Kamei N, Kawakami K, Takeda-Morishita M, Izawa H, Takechi-Haraya Y, et al. Dependence of Intestinal Absorption Profile of Insulin on Carrier Morphology Composed of β-Cyclodextrin-Grafted Chitosan. Molecular Pharmaceutics. 2016;13(12):4034-42.
37. Zhu X, Shan W, Zhang P, Jin Y, Guan S, Fan T, et al. Penetratin Derivative-Based Nanocomplexes for Enhanced Intestinal Insulin Delivery. Molecular Pharmaceutics. 2014;11(1):317-28.

38. Griffin BT, Guo J, Presas E, Donovan MD, Alonso MJ, O'Driscoll CM. Pharmacokinetic, pharmacodynamic and biodistribution following oral administration of nanocarriers containing peptide and protein drugs. Advanced Drug Delivery Reviews. 2016;106(Part B):367-80.
39. Zhang N, Ping Q, Huang G, Xu W, Cheng Y, Han X. Lectin-modified solid lipid nanoparticles as carriers for oral administration of insulin. International Journal of Pharmaceutics. 2006;327(1):153-9.
40. Fan T, Chen C, Guo H, Xu J, Zhang J, Zhu X, et al. Design and evaluation of solid lipid nanoparticles modified with peptide ligand for oral delivery of protein drugs. European Journal of Pharmaceutics and Biopharmaceutics. 2014;88(2):518-28.
41. Wang L, Yang Y-W, Zhu M, Qiu G, Wu G, Gao H. [small beta]-Cyclodextrin-conjugated amino poly(glycerol methacrylate)s for efficient insulin delivery. RSC Advances. 2014;4(13):6478-85.
42. Hui G, Yi-Nong W, Yun-Ge F, Jian-Biao M. Conjugates of poly(DL-lactide-co-glycolide) on amino cyclodextrins and their nanoparticles as protein delivery system. Journal of Biomedical Materials Research Part A. 2007;80A(1):111-22.